

Multi-isotope degeneracy of neutrinoless double- β decay mechanisms in the quasiparticle random-phase approximation

Amand Faessler,¹ G. L. Fogli,^{2,3} E. Lisi,³ A. M. Rotunno,² and F. Šimkovic^{4,5}

¹*Institute of Theoretical Physics, University of Tuebingen, 72076 Tuebingen, Germany*

²*Dipartimento Interateneo di Fisica “Michelangelo Merlin,” Via Amendola 173, 70126 Bari, Italy*

³*Istituto Nazionale di Fisica Nucleare, Sezione di Bari, Via Orabona 4, 70126 Bari, Italy*

⁴*Department of Nuclear Physics and Biophysics, Comenius University, Mlynská dolina F1, SK-842 15 Bratislava, Slovakia*

⁵*Bogoliubov Laboratory of Theoretical Physics, JINR, 141980 Dubna, Moscow Region, Russia*

(Received 21 March 2011; published 30 June 2011)

We calculate nuclear matrix elements of neutrinoless double beta decay ($0\nu\beta\beta$) in four different candidate nuclei (^{76}Ge , ^{82}Se , ^{100}Mo , ^{130}Te) within the quasiparticle random phase approximation and its uncertainties. We assume (up to) four coexisting mechanisms for $0\nu 2\beta$ decay, mediated by light Majorana neutrino exchange (ν), heavy Majorana neutrino exchange (N), R -parity breaking supersymmetry (R), and squark-neutrino (\tilde{q}), interfering either constructively or destructively with each other. We find that, unfortunately, current nuclear matrix element uncertainties appear to prevent a robust determination of the relative contribution of each mechanism to the decay amplitude, even assuming accurate measurements of decay lifetimes. The near-degeneracy of $0\nu\beta\beta$ mechanisms is analyzed with simple algebraic techniques, which do not involve assumptions about the statistical distribution of errors. We discuss implications of such degeneracy on prospective searches for absolute neutrino masses.

DOI: 10.1103/PhysRevD.83.113015

PACS numbers: 23.40.Hc, 12.60.Jv, 14.60.St, 21.60.Jz

I. INTRODUCTION

The discovery of neutrino masses and mixings [1] has given new impetus to the search for lepton number violation (LNV) and, in particular, for the process of neutrinoless double beta decay ($0\nu\beta\beta$) [2],

$$(Z, A) \rightarrow (Z + 2, A) + 2e^-, \quad (1)$$

in a variety of experiments using different (Z, A) nuclei [3]. The process can be mediated by light Majorana neutrinos, as well as by alternative (and possibly coexisting) mechanisms invoking new particles and interactions beyond the standard model [4].

In the case of a single LNV mechanism (labeled by an index j), the $0\nu\beta\beta$ decay half-life T_i in a given nucleus $i = (Z, A)$ reads

$$T_i^{-1} = G_i^j |M_i^j \eta_j|^2, \quad (2)$$

where G_i^j is a calculable phase-space factor, M_i^j is the $0\nu\beta\beta$ nuclear matrix element (NME), and η_j is a dimensionless LNV parameter, characteristic of the particle physics model. In the case of coexisting mechanisms with identical phase space ($G_i^j \equiv G_i$), the above expression is generalized as [5]

$$T_i^{-1} = G_i \left| \sum_j M_i^j \eta_j \right|^2. \quad (3)$$

In the above equation, the η_j parameters may take either sign (and, allowing CP violation, even complex phases), leading to constructive or destructive interference in the decay amplitude.

In the absence of independent constraints on the LNV parameters, the discrimination of different mechanisms requires that either the η_j 's are factorized out, or that they are determined through the data themselves. For instance, assuming one mechanism at a time, one may analyze η_j -independent ratios of half-life data $\{T_i\}$ from different nuclei (typically with a ^{76}Ge datum at denominator) [6–9], possibly including joint (T_i, T_k) probability distributions [10]. Alternatively, one may assume (at least) as many $\{T_i\}$ data as the number of considered mechanisms, and then solve Eq. (3) in terms of the η_j 's [5].

The studies in [8–10] suggest that, at least in principle, a few (possibly coexisting [5]) mechanisms may be discriminated with accurate half-life data, provided that the associated NME uncertainties in different nuclei are “small enough.” Attempts to quantify this statement in prospective scenarios have been made through Monte Carlo simulations with educated error guesses [9] or through likelihood analyses [10] including error covariances [11]. However, apart from the difficulty in estimating “ 1σ ” theoretical errors, the approaches in [9,10] had to rely upon a somewhat inhomogeneous comparison of NMEs taken from different publications or nuclear models; conversely, the NMEs in [5] were all calculated in the same model, but their variations were not fully included in the analysis, although it was noted that they could be relevant. In this work we adopt an approach where: (1) all NMEs and their variations are estimated with one and the same method, the quasiparticle random-phase approximation (QRPA [12]) and (2) the resulting discrimination of different mechanisms is analyzed with simple algebraic (rather than statistical) tools.

In particular, the effect of theoretical uncertainties is evaluated herein by varying several QRPA inputs, which require extensive NME calculations. As a consequence, our analysis is restricted to a relatively small set of candidate nuclei and mechanisms. We consider four among the experimentally promising [3] candidate nuclei, labeled by the index i :

$$i = {}^{76}\text{Ge}, {}^{82}\text{Se}, {}^{100}\text{Mo}, {}^{130}\text{Te}, \quad (4)$$

and four possible $0\nu\beta\beta$ decay processes, labeled by the index j ,

$$j = \nu, N, R, \tilde{q}, \quad (5)$$

corresponding to light Majorana neutrino exchange [13], heavy Majorana neutrino exchange [14–16], R -parity breaking supersymmetry mechanism [17–20], and squark-neutrino mechanism [21–23], respectively. We then study solutions to Eq. (3) in terms of prospective $\{T_i\}$ data. Unfortunately, we find that the reconstructed LNV parameters η_j of the four mechanisms to $0\nu\beta\beta$ decays are destabilized once different, currently admissible QRPA variants are considered. The effective degeneracy of mechanisms may have significant implications on the interpretation of upcoming $0\nu\beta\beta$ results, and on their interplay with other observations sensitive to absolute neutrino masses.

Our work is structured as follows. In Sec. II we describe the LNV mechanisms considered for $0\nu\beta\beta$ decay. In Sec. III we discuss relevant aspects of the nuclear structure calculations. In Sec. IV we analyze the problem of discriminating the mechanisms within QRPA uncertainties. In Sec. V we summarize our results and discuss their implications for absolute neutrino mass searches.

II. LNV MECHANISMS

In this section we describe relevant features of the four LNV mechanisms in Eq. (5). In each i th nucleus [Eq. (4)], they share the same phase space G_i , estimated in [16] as

$$\begin{aligned} G({}^{76}\text{Ge}, {}^{82}\text{Se}, {}^{100}\text{Mo}, {}^{130}\text{Te}) \\ = (7.93, 35.2, 57.3, 55.4) \times 10^{-15} \text{y}^{-1}. \end{aligned} \quad (6)$$

Conventionally, the above phase-space factors embed the fourth power of the axial-coupling constant at the fixed value $g_A = 1.25$, and the inverse square of the nuclear radius $R = r_0 A^{1/3}$, with fixed $r_0 = 1.1$ fm. They are compensated by factors $(g_A/1.25)^2$ and $1/R$ in the definition of the matrix elements M_i^j [24].

A. Light Majorana neutrino exchange (ν)

In the usual case of exchange of three light Majorana neutrinos ν_h (with masses m_h , Majorana phases ϕ_h , and ν_e mixings U_{eh}), the LNV parameter takes the well-known form

$$\eta_\nu = \sum_{h=1}^3 |U_{eh}|^2 e^{i\phi_h} \frac{m_h}{m_e} \equiv \frac{m_{\beta\beta}}{m_e}, \quad (7)$$

where m_e is the electron mass, and $m_{\beta\beta}$ is the ‘‘effective Majorana mass.’’ In each nucleus, the nuclear matrix element M^ν consists of Fermi (F), Gamow-teller (GT) and tensor (T) contributions,

$$M^\nu = \left(\frac{g_A}{1.25}\right)^2 \left(M_{\text{GT}}^\nu + M_{\text{T}}^\nu - \frac{M_{\text{F}}^\nu}{g_A^2}\right), \quad (8)$$

with F, GT, and T operators defined as in [16,25].

B. Heavy Majorana neutrino exchange (N)

The neutrino mass spectrum may include, in principle, any number of heavy Majorana states N_k with masses M_k above the typical $0\nu\beta\beta$ energy scale, i.e., greater than $O(10)$ GeV. We restrict our consideration to the case of right-handed Majorana fermions, which are singlets of the $\text{SU}_L(2) \times \text{U}(1)$ group. Then, heavy neutrinos can mediate $0\nu\beta\beta$ decay with a LNV parameter η_N given by

$$\eta_N = \sum_k^{\text{heavy}} |U_{ek}|^2 e^{i\Phi_k} \frac{m_p}{M_k}, \quad (9)$$

where m_p is the proton mass, while the U_{ek} are the mixing matrix elements associated to left-handed weak interactions. Also in this case, the nuclear matrix element M^N is of the form

$$M^N = \left(\frac{g_A}{1.25}\right)^2 \left(M_{\text{GT}}^N + M_{\text{T}}^N - \frac{M_{\text{F}}^N}{g_A^2}\right), \quad (10)$$

with F, GT, and T operators discussed at length in [16].

C. R -parity breaking mechanism (R)

In supersymmetric (SUSY) models one may define a multiplicative quantum number $R = (-1)^{2S+3B+L}$ (with S, B, and L being the spin, baryon, and lepton numbers), which takes the value +1 for ordinary particles, and -1 for their superpartners. R -parity breaking allows (among others) superpotential terms of the form $W_{\tilde{R}} \ni \lambda'_{ijk} L_i Q_j D_k^c$, where L and Q are lepton and quark doublet left-handed superfields, D^c is a down quark singlet superfield, and λ' is a trilinear coupling. These terms can trigger $0\nu\beta\beta$ decay with short-range exchange of heavy superpartners (see below in this subsection) and with long-range exchange of heavy squarks plus light neutrinos (see the next subsection).

Assuming a dominant, short-range exchange of a heavy gluino with mass $m_{\tilde{g}}$, the LNV parameter $\eta_{\tilde{R}}$ takes a simplified form, symmetric in the masses of the u and d squarks:

$$\eta_{\dot{K}} = \frac{\pi\alpha_s}{6} \frac{(\lambda'_{111})^2}{G_F^2} \frac{m_p}{m_{\tilde{g}}} \frac{(m_{\tilde{u}_L}^2 + m_{\tilde{d}_R}^2)^2}{m_{\tilde{u}_L}^4 \cdot m_{\tilde{d}_R}^4}, \quad (11)$$

where G_F is the Fermi constant and α_s the strong coupling constant. At hadron level, in the hypothesis of one-pion and two-pion exchange dominance, the matrix element contains both tensor and Gamow-Teller contributions,

$$M^{\dot{K}} = \left(\frac{g_A}{1.25}\right)^2 [c^{1\pi}(M_{\text{T}}^{1\pi} + M_{\text{GT}}^{1\pi}) + c^{2\pi}(M_{\text{T}}^{2\pi} + M_{\text{GT}}^{2\pi})], \quad (12)$$

with known prefactors $c^{1\pi}$ and $c^{2\pi}$. See [20,26] for further details.

D. Squark-neutrino mechanism (\tilde{q}).

R -parity breaking SUSY may trigger $0\nu\beta\beta$ decay via long-range exchange of (not necessarily massive) neutrinos plus squarks [27]. The corresponding LNV parameter is sensitive to down-squark ($\tilde{d}_{(k)} = \tilde{d}, \tilde{s}, \tilde{b}$) masses and left-right mixings:

$$\eta_{\tilde{q}} = \sum_k \frac{\lambda'_{11k}\lambda'_{1k1}}{2\sqrt{2}G_F} \sin 2\theta_{(k)}^d \left(\frac{1}{m_{\tilde{d}_{1(k)}}^2} - \frac{1}{m_{\tilde{d}_{2(k)}}^2} \right). \quad (13)$$

At hadron level, in the hypothesis of pion-exchange dominance, the matrix element contains both tensor and Gamow-Teller contributions, with a resulting matrix element of the form

$$M^{\tilde{q}} = \left(\frac{g_A}{1.25}\right)^2 (M_{\text{GT}}^{\pi} - M_{\text{T}}^{\pi}). \quad (14)$$

See [27] for further details.

E. Remarks on ν , N , R , \tilde{q} mechanisms

The above four mechanisms are different in several respects: light and heavy neutrino exchange NMEs do not exactly scale as g_A^2 (because of Fermi contributions), unlike SUSY mechanisms, which also have large tensor contributions; moreover, short-range mechanisms (such as heavy neutrino exchange) are particularly sensitive to the nucleon-nucleon potential. Thus, one might expect to find different NME isotopic patterns in different mechanisms. However, we shall see in Sec. IV that the resulting differences in NME patterns are comparable to current QRPA variations, thus preventing an effective discrimination of the mechanisms based on multi-isotope $0\nu\beta\beta$ half-life data.

The similarity of NME patterns in the different nuclei and mechanisms considered herein suggests that nucleon (rather than nuclear) physics dominates in all cases. For the ν mechanism, the dominance of short-range nucleon-nucleon contributions has been shown in different approaches [25,28,29]. It would be useful to perform similar studies for nonstandard mechanisms as well.

III. NUCLEAR STRUCTURE CALCULATIONS

In what follows, the $0\nu\beta\beta$ nuclear matrix elements M_i^j are evaluated (for $i = {}^{76}\text{Ge}, {}^{82}\text{Se}, {}^{100}\text{Mo}, {}^{130}\text{Te}$ and $j = \nu, N, R, \tilde{q}$) under the so-called self-consistent renormalized QRPA (SRQRPA) [30–32], which takes into account the Pauli exclusion principle and conserves the mean particle number in correlated ground states. The following variants are introduced to account for intrinsic QRPA uncertainties.

For each nucleus, two choices of single-particle basis are considered: intermediate and large. The intermediate-size model space (m.s.) has 12 levels (oscillator shells $N = 2-4$) for ${}^{76}\text{Ge}, {}^{82}\text{Se}$, 16 levels (oscillator shells $N = 2-4$ plus the $f + h$ orbits from $N = 5$) for ${}^{100}\text{Mo}$ and 18 levels (oscillator shells $N = 3, 4$ plus $f + h + p$ orbits from $N = 5$) for ${}^{130}\text{Te}$. The large-size single-particle space contains 21 levels (oscillator shells $N = 0-5$) for ${}^{76}\text{Ge}, {}^{82}\text{Se}, {}^{100}\text{Mo}$, and 23 levels ($N = 1-5$ and i orbits from $N = 6$) for ${}^{130}\text{Te}$. In comparison with previous studies [24] we omit the small-size model space, as it is insufficient to describe realistically the tensor matrix elements.

The single-particle energies are obtained by using a Coulomb-corrected Woods-Saxon potential. Two-body G -matrix elements are derived from the Argonne and the Charge Dependent Bonn (CD-Bonn) one-boson exchange potential within the Brueckner theory. The schematic pairing interactions are adjusted to fit the empirical pairing gaps [33]. The particle-particle and particle-hole channels of the G -matrix interaction of the nuclear Hamiltonian H are renormalized by introducing the parameters g_{pp} and g_{ph} , respectively. The calculations are been carried out for $g_{ph} = 1.0$.

The particle-particle strength parameter g_{pp} of the SRQRPA is fixed by the data on the two-neutrino double beta ($2\nu\beta\beta$) decays [24]. In the calculation of the $0\nu\beta\beta$ -decay NMEs, we consider the two-nucleon short-range correlations derived from the Argonne or CD-Bonn nucleon-nucleon (NN) potentials as residual interactions [34]. The measured $2\nu\beta\beta$ -decay half-lives $T_{2\nu}$, taken from [35], fix the matrix element $|M_{\text{GT}}^{2\nu}|$ via $T_{2\nu}^{-1} = G_{2\nu}g_A^4 |m_e M_{\text{GT}}^{2\nu}|^2$, where $G_{2\nu}$ is the g_A -independent phase-space factor for $2\nu\beta\beta$ decay. The value of g_{pp} is thus fixed for any given g_A , which we take equal to either its bare value ($g_A = 1.25$) or its quenched value ($g_A = 1.00$) for all nuclei. For simplicity, we neglect the possibility of different g_A quenching in different nuclei [36]. Finally, for each $2\nu\beta\beta$ constraint to g_{pp} , we take both the $T_{2\nu}$ central value and its $\pm 1\sigma$ deviations, leading to a triplet of g_{pp} estimates (best fit $\pm 1\sigma$) in each case.

Summarizing, our analysis is based on the calculation of 384 NMEs, corresponding to four nuclei (i), four mechanisms (j), two model space sizes (m.s.), two nucleon-nucleon potentials (NN), two axial-coupling values (g_A), and three particle-particle strength values (g_{pp}),

$$384(\text{NME}) = 4(i) \times 4(j) \times 2(\text{m.s.}) \times 2(NN) \\ \times 2(g_A) \times 3(g_{pp}). \quad (15)$$

However, we have verified *a posteriori* that g_{pp} variations within $\pm 1\sigma$ induce NME variations much smaller than those induced by changes in model space, nucleon potential, or g_A . The analysis discussed in the next section turns out to be basically unaffected by such extra g_{pp} variations. In what follows, we shall thus focus on the numerical results obtained at the central values for the g_{pp} 's. In particular, we restrict our analysis to eight 4×4 matrices M_i^j of NME's, corresponding to eight QRPA variants,

TABLE I. Matrices M_i^j of NMEs for $i = ({}^{76}\text{Ge}, {}^{82}\text{Se}, {}^{100}\text{Mo}, {}^{130}\text{Te})$ and $j = (\nu, N, R, \bar{q})$, for each of the 8 variants adopted within the QRPA. The $2 \times 2 \times 2 = 8$ variants correspond to different choices for the model space size (intermediate or large), for the NN potential (Argonne or CD-Bonn), and for the g_A value (1 or 1.25).

QRPA case	$i \setminus j$	ν	N	R	\bar{q}
Variant n. 1: $g_A = 1$, $NN = \text{Argonne}$, $\text{m.s.} = \text{intermediate}$	${}^{76}\text{Ge}$	3.85	172	387	396
	${}^{82}\text{Se}$	3.59	165	375	379
	${}^{100}\text{Mo}$	3.62	185	412	405
	${}^{130}\text{Te}$	3.29	171	385	382
Variant n. 2: $g_A = 1$, $NN = \text{Argonne}$, $\text{m.s.} = \text{large}$	${}^{76}\text{Ge}$	4.40	196	461	476
	${}^{82}\text{Se}$	4.19	193	455	465
	${}^{100}\text{Mo}$	3.91	192	450	449
	${}^{130}\text{Te}$	3.34	177	406	403
Variant n. 3: $g_A = 1$, $NN = \text{CD-Bonn}$, $\text{m.s.} = \text{intermediate}$	${}^{76}\text{Ge}$	4.15	269	340	408
	${}^{82}\text{Se}$	3.86	259	329	390
	${}^{100}\text{Mo}$	3.96	299	356	416
	${}^{130}\text{Te}$	3.64	277	336	397
Variant n. 4: $g_A = 1$, $NN = \text{CD-Bonn}$, $\text{m.s.} = \text{large}$	${}^{76}\text{Ge}$	4.69	317	393	483
	${}^{82}\text{Se}$	4.48	312	388	472
	${}^{100}\text{Mo}$	4.20	311	384	455
	${}^{130}\text{Te}$	3.74	294	350	416
Variant n. 5: $g_A = 1.25$, $NN = \text{Argonne}$, $\text{m.s.} = \text{intermediate}$	${}^{76}\text{Ge}$	4.75	233	587	594
	${}^{82}\text{Se}$	4.54	226	574	578
	${}^{100}\text{Mo}$	4.40	250	629	612
	${}^{130}\text{Te}$	4.16	234	595	589
Variant n. 6: $g_A = 1.25$, $NN = \text{Argonne}$, $\text{m.s.} = \text{large}$	${}^{76}\text{Ge}$	5.44	265	700	718
	${}^{82}\text{Se}$	5.29	263	698	710
	${}^{100}\text{Mo}$	4.79	260	690	683
	${}^{130}\text{Te}$	4.18	240	626	620
Variant n. 7: $g_A = 1.25$, $NN = \text{CD-Bonn}$, $\text{m.s.} = \text{intermediate}$	${}^{76}\text{Ge}$	5.11	351	515	612
	${}^{82}\text{Se}$	4.88	340	504	595
	${}^{100}\text{Mo}$	4.81	388	544	628
	${}^{130}\text{Te}$	4.62	364	519	611
Variant n. 8: $g_A = 1.25$, $NN = \text{CD-Bonn}$, $\text{m.s.} = \text{large}$	${}^{76}\text{Ge}$	5.82	412	596	728
	${}^{82}\text{Se}$	5.66	408	594	720
	${}^{100}\text{Mo}$	5.15	404	589	691
	${}^{130}\text{Te}$	4.70	384	540	641

associated to changes in model space size, NN potential, and g_A ,

$$8(M_i^j) = 2(\text{m.s.}) \times 2(NN) \times 2(g_A). \quad (16)$$

Table I reports the corresponding M_i^j estimates with three significant digits.

IV. DISCRIMINATION OF MECHANISMS: EXPECTATIONS AND RESULTS

The system of equations in (3) involves, in general, four unknown complex parameters η_j . For the sake of simplicity, as in [5], we restrict ourselves to a CP -conserving scenario with real η_j . The relative sign of the η_j 's can, however, be positive or negative, leading to constructive or destructive interference among different mechanisms. Taking square roots in Eq. (3) leads to a further \pm sign ambiguity for each index i [5]. We restrict our analysis to the case with all “+” signs for each i , namely, to the linear system of equations

$$\sum_{j=1}^4 M_i^j \eta_j = \mu_i (i = 1, \dots, 4), \quad (17)$$

where

$$\mu_i = (G_i T_i)^{-1/2}. \quad (18)$$

Relaxing the above simplifying assumptions would corroborate the results which follow.

A. Expectations

For given multi-isotope data $\{T_i\}$, solutions to the linear system in Eq. (17) in terms of $\{\eta_j\}$ should identify, in principle, the underlying physics mechanism(s) [5]. Testing different mechanisms, as well as their possible coexistence, becomes then a parameter estimation problem in η_j -space, provided that theoretical uncertainties (for M_i^j) and experimental errors (for T_i) are accounted for. For instance, if $0\nu\beta\beta$ decays were due only to light Majorana neutrino exchange, accurate solutions to Eq. (17) should ideally cluster around a point $(\langle\eta_\nu\rangle, 0, 0, 0) \simeq (\langle\eta_\nu\rangle, 0, 0, 0)$. Conversely, nonzero values for two or more η_j 's would signal the coexistence of two or more mechanisms in $0\nu\beta\beta$ decay. This approach has been discussed in [5] where, however, the NME values were taken from a single QRPA calculation with fixed input parameters, whose possible variations were not considered.

As we show below, it turns out that the solutions $\{\eta_j\}$ are destabilized once QRPA variants are accounted for, even in the presence of accurate measurements ($\delta T_i/T_i \ll 1$). In particular, the linear system of Eq. (17) is shown to be ill-conditioned, with matrices M_i^j of nearly rank one, leading to an effective degeneracy of mechanisms. Before dealing with the M_i^j algebra, it is useful to illustrate the source of such degeneracy in a graphical way.

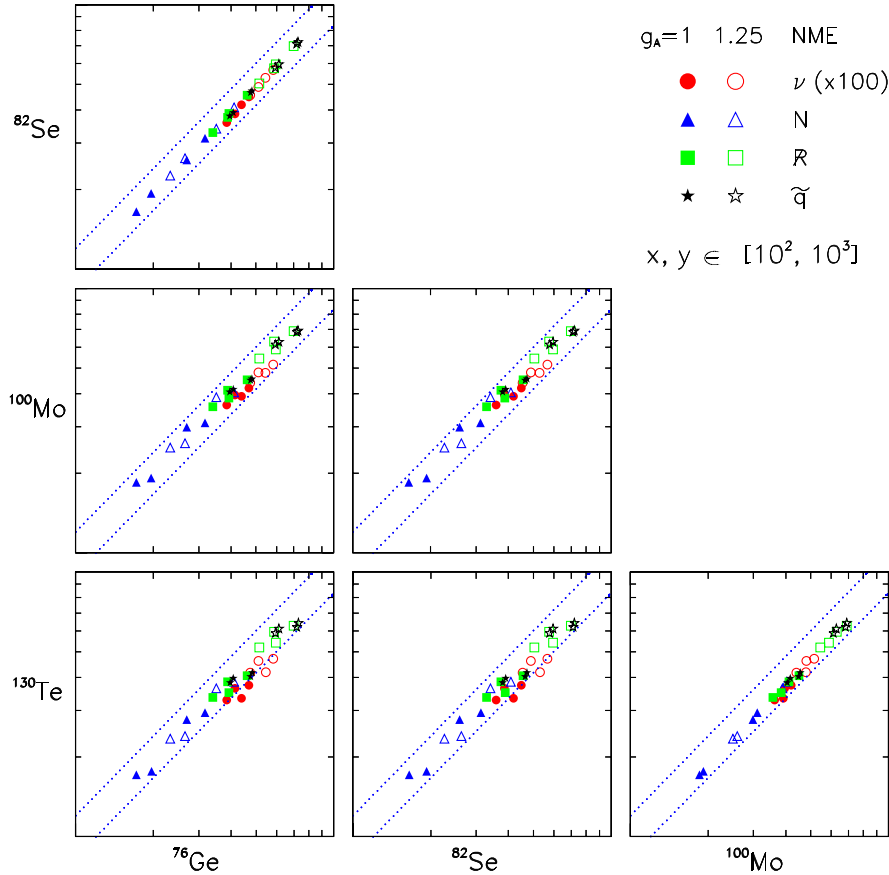
$0\nu\beta\beta$ NME scatter plot


FIG. 1 (color online). Graphical representation of the NMEs in Table I as a scatter plot, for each couple of nuclei among ^{76}Ge , ^{82}Se , ^{100}Mo , and ^{130}Te . Eight QRPA variants are shown for each of the four different $0\nu\beta\beta$ mechanisms, labeled as ν (circles), N (triangles), R (squares), and \tilde{q} (stars). Solid and empty markers refer to $g_A = 1$ and $g_A = 1.25$, respectively. In each panel, the (x, y) coordinates span the range $[10^2, 10^3]$ in logarithmic scale. For the ν mechanism, NMEs are scaled ($\times 100$) to fit the range. Diagonal dotted lines mark the band where the x and y coordinates differ by up to 20%. The NMEs appear to cluster along the diagonals, suggesting an effective degeneracy of the $0\nu\beta\beta$ mechanisms. See the text for details.

Figure 1 shows the contents of Table I as a scatter plot of NMEs, for each couple of nuclei among ^{76}Ge , ^{82}Se , ^{100}Mo , and ^{130}Te . For each mechanism, the eight QRPA variants correspond to eight markers (circles for ν , triangles for N , squares for R , and stars for \tilde{q}), solid and empty markers corresponding to $g_A = 1$ and $g_A = 1.25$, respectively. NMEs for the ν mechanism are multiplied by a factor of 100 in order to fit in the chosen logarithmic scales, which span the range $[10^2, 10^3]$. Note that, on such scales, the effects of g_{pp} variations mentioned in Sec. III would be unobservable. Diagonal dotted lines mark the band where the x and y coordinates are equal up to 20%. The source of degeneracy is then rather clear: all NMEs cluster along the diagonal in each panel, with little spread (less than about 20%) in the orthogonal direction. In particular, the transverse spread induced by different mechanisms appears to be comparable to that induced by the QRPA variants. In other words, the columns of the M_i^j matrices are roughly proportional to each other, and with comparable entries for

different nuclei, within QRPA uncertainties. The linear system in Eq. (17) is then expected to be significantly degenerate, with nearly “null determinant” not only for the full 4×4 matrix M_i^j , but also for all of its 3×3 and 2×2 submatrices. These expectations are confirmed by the following numerical arguments.

B. Numerical results

Stability and degeneracy issues in linear equation systems are best dealt with the singular value decomposition (SVD) technique [37,38]. For a square matrix \mathbf{M} as in Eq. (17) the SVD is equivalent to diagonalizing the product matrix $\mathbf{M} \cdot \mathbf{M}^T$, taking the square roots of the eigenvalues, and sorting them in descending order. The resulting set of “singular values” σ_i encodes relevant information on the stability of solutions [37,38]. In fact, if all σ_i 's have comparable magnitudes, the η_j solutions to Eq. (17) tend to be stable under small variations in either the M_i^j or μ_i

entries. Conversely, if at least one σ_i is much smaller than the others, the system is ill-conditioned and generates unstable solutions. In particular, an ill-conditioned system, characterized by a large “condition number” $\kappa = \sigma_{\max}/\sigma_{\min}$, is expected to become unstable when the fractional variations δM_i^j or $\delta \mu_i$ become comparable to the reciprocal condition number $\rho = 1/\kappa$ [37,38]. A slightly more technical point concerns the optimization of ρ . Although ρ is invariant under an overall scaling of matrix entries ($M_i^j \rightarrow f \cdot M_i^j$), it may change under separate scalings of rows and columns ($M_i^j \rightarrow r_i \cdot M_i^j \cdot s_j$), which transform Eq. (17) into an equivalent system, provided that $\eta_j \rightarrow \eta_j/s_j$ and $\mu_i = \mu_i \cdot s_i$. The maximization of ρ by row/column rescalings, usually called “matrix equilibration” [37–39], provides more robust estimates of the fractional errors which may trigger unstable solutions. Summarizing, the SVD of an equilibrated matrix provides useful information about the effective matrix rank (equal to the number of “large” singular values) and about the size of “dangerous” fractional errors (equal to the reciprocal condition number ρ).

Table II reports the singular values and (reciprocal) condition numbers, as obtained by applying equilibration and SVD routines [39] to the eight matrices M_i^j in Table I. In each of the eight QRPA variants, only one singular value is of $O(1)$, the others being smaller by one to 3 orders of magnitude. The matrices M_i^j are thus nearly of rank one, leading to basically undetermined and degenerate solutions. Instabilities of solutions to Eq. (17) are expected to arise already for δM_i^j as small as $\rho \sim O(10^{-3})$, implying that even three-digit approximations are potentially dangerous.

Let us discuss a representative numerical check, by assuming a scenario with true NMEs taken from the first matrix of Table I, and true LNV parameters ($\eta_\nu, \eta_N, \eta_{\hat{R}}, \eta_{\hat{q}}$) set to $(6.18 \times 10^{-7}, 0, 0, 0)$, corresponding to a single $0\nu\beta\beta$ mechanism, namely, light Majorana neutrino exchange with $m_{\beta\beta} = 0.316$ eV. Such choices for M_i^j and η_j imply the following μ_i values (up to three significant digits):

TABLE III. Relative contribution W_j of the j th $0\nu\beta\beta$ mechanism to the total ^{76}Ge decay amplitude ($\sum_j W_j = 1$), for eight QRPA variants, assuming $W_j = \delta_{j1}$ as true case, and precisely known lifetimes T_i for the four nuclei (see the text for details).

Variant	W_ν	W_N	$W_{\hat{R}}$	$W_{\hat{q}}$
1	+1.05	−0.01	+0.12	−0.16
2	+3.14	+5.62	−1.05	−6.71
3	+1.26	−0.24	+0.94	−0.96
4	+3.83	+2.63	+2.13	−7.59
5	+1.00	+3.07	−2.83	−0.24
6	+7.90	+16.22	+1.86	−24.98
7	+1.97	+1.09	−0.27	−1.79
8	+6.64	+5.90	+5.99	−17.53

$$\mu(^{76}\text{Ge}, ^{82}\text{Se}, ^{100}\text{Mo}, ^{130}\text{Te}) = (2.38, 2.22, 2.24, 2.03) \times 10^{-6}, \quad (19)$$

and a ^{76}Ge half-life of 2.23×10^{25} y, which purposely reproduces the claimed measurement in [40,41]. With the above μ_i 's, we solve Eq. (17) in the unknowns η_j for each of the eight matrices in Table I, including the first one (where we expect to recover the “true” η_j by construction).

Table III shows the results of our exercise, in terms of the relative contribution W_j of each j -th mechanism to the $0\nu\beta\beta$ amplitude in ^{76}Ge ($i = 1$),

$$W_j = \frac{M_1^j \eta_j}{\sum_{j=1}^4 M_1^j \eta_j} \Rightarrow \sum_{j=1}^4 W_j = 1. \quad (20)$$

In the first row of Table III, one would expect to recover the true ν mechanism, corresponding to $W_\nu = 1$ and $W_{N,\hat{R},\hat{q}} = 0$. However, this is not the case: the three-digit approximation is already sufficient to generate spurious contributions (e.g., $W_{\hat{q}} = -0.16$). In the second to eighth row in Table III, where QRPA variants entail relative variations $\delta M_i^j \gg O(10^{-3})$, disparate solutions emerge, with constructive or destructive interference of (sub)dominant

TABLE II. Singular value decomposition of the (equilibrated) matrices M_i^j given in Table I. For each of the eight QRPA variants, we report the four singular values σ_i (in descending order), the matrix condition number κ , and the reciprocal condition number $\rho = 1/\kappa$. The inequality $\sigma_1 \gg \sigma_{2,3,4}$ signals that each matrix M_i^j is ill-conditioned and nearly threefold degenerate. See the text for details.

Variant	$\sigma_1 = \sigma_{\max}$	σ_2	σ_3	$\sigma_4 = \sigma_{\min}$	$\kappa = \sigma_{\max}/\sigma_{\min}$	$\rho = \sigma_{\min}/\sigma_{\max}$
1	3.91	9.92×10^{-2}	14.3×10^{-3}	4.71×10^{-3}	0.83×10^3	1.20×10^{-3}
2	3.91	9.66×10^{-2}	7.46×10^{-3}	3.40×10^{-3}	1.15×10^3	0.87×10^{-3}
3	3.89	9.66×10^{-2}	21.4×10^{-3}	3.50×10^{-3}	1.11×10^3	0.90×10^{-3}
4	3.91	8.26×10^{-2}	13.6×10^{-3}	3.58×10^{-3}	1.09×10^3	0.92×10^{-3}
5	3.91	10.6×10^{-2}	14.3×10^{-3}	2.86×10^{-3}	1.37×10^3	0.73×10^{-3}
6	3.91	10.0×10^{-2}	8.20×10^{-3}	1.28×10^{-3}	3.05×10^3	0.33×10^{-3}
7	3.89	10.0×10^{-2}	17.3×10^{-3}	5.74×10^{-3}	0.68×10^3	1.48×10^{-3}
8	3.91	8.68×10^{-2}	16.9×10^{-3}	2.04×10^{-3}	1.92×10^3	0.52×10^{-3}

mechanisms. For instance, in the eight row, three large coherent contributions from the ν , N , and R mechanism are almost cancelled by an even larger opposite contribution by the \tilde{q} mechanism. In Table III, the largest amplitude corresponds to W_ν in only two cases (1st and 3rd variant), while in others it corresponds to either W_N (5th variant) or $W_{\tilde{q}}$ (remaining variants).

Note that the instability of the W_j 's (in both magnitude and sign) arises from intrinsic properties of the NME matrices M_i^j and would be present also for other choices of the true LNV parameters (e.g. by assuming another mechanism as dominant). Moreover, varying input data in Eq. (19) within prospective errors, as well as removing the simplifying assumptions preceding Eq. (17), would only generate further instabilities or multiplicities in the solutions.

If the problem is reduced to just three or two mechanisms (instead of four), the instabilities, although less severe, remain harmful. In generic 3×3 and 2×2 minors of the M_i^j matrices, unstable solutions are expected to arise for fractional variations δM_i^j of order $\rho_3 = \sigma_3/\sigma_1 \sim \text{few} \times 10^{-3}$ and $\rho_2 = \sigma_2/\sigma_1 \sim \text{few} \times 10^{-2}$, respectively. Since current QRPA variants induce $\delta M_i^j \sim O(10^{-1})$, a robust reconstruction of the true scenario cannot be achieved.

As a numerical check, we have repeated the previous exercise in the subcase (^{76}Ge , ^{130}Te) \times (ν , \tilde{q}), which is among the ‘‘less degenerate’’ 2×2 ones. We find reciprocal condition numbers $\rho_{2 \times 2} \simeq \text{few}\%$, as expected. Since QRPA variants entail $\delta M_i^j \sim O(10^{-1})$, solutions are unstable, and the reconstruction of true case ($W_\nu = 1$) yields fake values for W_ν , ranging from a minimum of 0.23 (corresponding to dominant \tilde{q} mechanism) to a maximum of 1.5 (corresponding to destructive interference of ν and \tilde{q} mechanisms). If we further change either $\mu(^{76}\text{Ge})$ or $\mu(^{130}\text{Te})$ by $\pm 10\%$ (corresponding to $\pm 20\%$ experimental uncertainties in $0\nu\beta\beta$ half-lives), we find reconstructed values of W_ν within a wider interval, $W_\nu \in [-1.4, +2.9]$. This range spans disparate solutions, including coexisting ν and \tilde{q} mechanisms with constructive or destructive interference, as well as subcases close to single ν or single \tilde{q} mechanism ($W_\nu \simeq 1$ or $W_{\tilde{q}} \simeq 1$, respectively). Analogous results hold for other 2×2 minors. Note that, since the M_i^j matrices are nearly of rank one ($\sigma_1 \gg \sigma_{2,3,4}$), the degeneracy applies to rectangular submatrices as well; thus, the situation would not significantly improved by overconstraining the system, e.g., by forcing two mechanisms to (approximately) fit more than two lifetime data among those considered.

We stress that the observed degeneracy derives from the nearly threefold singularity of the matrices M_i^j , and not from specific choices of prospective input data μ_i or of true LNV parameters η_j . The phenomenological indistinguishability of the (ν , N , R , \tilde{q}) mechanisms in the (^{76}Ge , ^{82}Se , ^{100}Mo , ^{130}Te) nuclei appears to be an unfortunate but

general result, as far as the current QRPA framework and its estimated variants [leading to $\delta M_i^j \sim O(10^{-1})$] are assumed. The numerical analysis suggests a very ambitious accuracy goal for prospective QRPA estimates [i.e., a relative spread δM_i^j at the few percent level], in order to clearly discriminate the relative contributions of two mechanisms by means of two nuclei, among those considered herein.

C. Discussion

The difficulty of separating the ν mechanism from heavy Majorana neutrino exchange or from SUSY-mediated decays in multi-isotope $0\nu\beta\beta$ data had been noted earlier in [8–10]. The results presented in this work corroborate such findings, with the advantage of being based on a homogeneous comparison of NMEs, calculated in well-defined variants of one and the same nuclear model, for all the nuclei and mechanisms considered—which was not the case in [8–10]. Therefore, the emerging degeneracy appears to be quite general and not accidental, in the context of the considered mechanisms: for any of them, the NMEs turn out to have a similar size in the various nuclei, with uncertainties mostly absorbed by common scaling factors. The resulting numerical degeneracy in the determination of LNV parameters is supported and quantified by simple algebraic arguments, which do not assume specific distributions of theoretical errors. As such, the analysis method could be extended to other nuclei, mechanisms or nuclear structure models.

Taken together, the results of [8–10] and of this paper show, from different viewpoints, that $0\nu\beta\beta$ mechanisms mediated by (light or heavy) neutrino exchange and by R supersymmetry may be phenomenologically degenerate in some nuclei of interest, within realistic uncertainties. Therefore, $0\nu\beta\beta$ signals or limits from such nuclei could be generically interpreted in terms of unconstrained linear combinations of coexisting (ν , N , R , \tilde{q}) mechanisms, including subcases with one dominant (if not single) mechanism. Breaking the degeneracy would require significantly more accurate NME estimates than can be obtained in current, state-of-the-art QRPA.

It should also be noted that we have considered only CP -conserving cases [i.e., real μ_i in Eq. (17)] and, furthermore, we have discarded the discrete ambiguities related to the two possible signs for each index i ($\mu_i \rightarrow \pm \mu_i$) [5], which would worsen the degeneracy problem by increasing the multiplicity of solutions. In CP -violating scenarios, with unknown relative phases ϕ_i among different $0\nu\beta\beta$ decay amplitudes, the discrete ambiguities would become continuous ($\mu_i \rightarrow e^{i\phi_i} \mu_i$), thus rendering the system in Eq. (17) undetermined, unless extra independent data were added to constrain the unknowns ϕ_i . In any case, removal of our simplifying assumptions about the CP properties of the μ_i parameters would make the degeneracy problem more (not less) difficult to solve.

These negative findings do not exclude, of course, more favorable scenarios in other nuclei or mechanisms. For instance, it has been noted in [8–10] that left-right symmetric models with hadronic right-handed currents have better chances to be distinguished from ν exchange via multi-isotope half-life data. Extra-dimensional models with Kaluza-Klein neutrino states may also provide phenomenologically distinctive patterns [8]. Moreover, additional information from angular and energy electron distributions in the final state might help breaking degeneracies (see, e.g., [42]). The analysis of further (potentially more promising) mechanisms and observables, and of their relative discrimination in the presence of theoretical variants, is left to future works.

A final remark is in order. Besides the QRPA framework adopted in this work, other independent approaches have been (and are being) adopted in the calculation of NMEs for different nuclei, especially in the reference case of light Majorana neutrino exchange. Recent notable contributions include, e.g., applications of the large scale shell model (LSSM) [43], of the interacting boson model (IBM) [44], of the projected Hartree-Fock-Bogoliubov method (PHFB) [45], and of the energy density functional method (EDF) [46]; see the review in [47]. The comparison of results obtained with these and other methods (or their variants) shows that the current spread of independent, state-of-the-art NME calculations exceeds the uncertainties estimated within the QRPA approach alone [47], suggesting that further efforts are needed to constrain various theoretical approximations and systematics. These efforts, which would be boosted by future experimental observations of $0\nu\beta\beta$ decay, will certainly help to understand better the source(s) of the degeneracy discussed in this work and, hopefully, to reduce the NME uncertainties at values small enough to allow the discrimination of at least two mechanisms.

V. SUMMARY AND IMPLICATIONS

We have considered nuclear matrix elements for neutrinoless double beta decay in four nuclei (^{76}Ge , ^{82}Se , ^{100}Mo , ^{130}Te), within the self-consistent renormalized QRPA approach, for four $0\nu 2\beta$ decay mechanisms, mediated by light Majorana neutrino exchange (ν), heavy Majorana neutrino exchange (N), R -parity breaking supersymmetry (R), and squark-neutrino (\tilde{q}). QRPA uncertainties have been evaluated by changing the model space size, the nucleon-nucleon potential, and the axial coupling. We have found that, within current QRPA uncertainties, the four mechanisms appear to be largely degenerate, and could coexist in phenomenologically indistinguishable linear combinations (regardless of experimental errors and of possible complex phases). The degeneracy analysis is based on simple algebraic (rather than statistical) tools, which could be extended to NME estimates for other nuclei or mechanisms.

As far as the degeneracy in the (^{76}Ge , ^{82}Se , ^{100}Mo , ^{130}Te) nuclei is concerned, one could, e.g., interpret their $0\nu\beta\beta$ decay rates in terms of an effective phenomenological parameter of the form

$$m'_{\beta\beta} \simeq m_{\beta\beta} + \Delta m_{\beta\beta}, \quad (21)$$

where $m_{\beta\beta}$ is the usual effective Majorana mass for light ν exchange, while $\Delta m_{\beta\beta}$ embeds possible extra contributions from the (N , R , \tilde{q}) mechanisms, with either constructive ($\Delta m_{\beta\beta} > 0$) or destructive ($\Delta m_{\beta\beta} < 0$) interference with the ν mechanism. Note that, in the hypothetical case of nearly exact destructive interference ($m'_{\beta\beta} \simeq 0$), the process of $0\nu\beta\beta$ decay might be strongly suppressed and even escape observation in the four nuclei, despite the presence of Majorana neutrinos with $m_{\beta\beta} > 0$.

A nonstandard degree of freedom $\Delta m_{\beta\beta}$ could be relevant in comparing $0\nu\beta\beta$ results with other searches for absolute ν masses, such as β -decay (probing $m_{\beta}^2 = \sum_h |U_{eh}|^2 m_h^2$) and precision cosmology (probing $\Sigma = m_1 + m_2 + m_3$), especially if conflicting data emerge. An example is suggested by current results. Roughly speaking, for nearly degenerate neutrino masses ($m_{1,2,3} \simeq m_\nu$) it is $\Sigma \simeq 3m_\nu$, with typical cosmological constraints ($\Sigma \lesssim 0.6$ eV [48]) placing the upper bound $m_\nu \lesssim 0.2$ eV. Assuming only the standard ν mechanism, one has $m_{\beta\beta} \simeq m_\nu f$ ($f \in [0.38, 1]$) which, if $m_{\beta\beta} \sim 0.3$ eV is inferred from the claim in [40,41], translates into a lower bound $m_\nu \simeq m_{\beta\beta}/f \gtrsim 0.3$ eV. This well-known tension [48] could be relaxed by interpreting the $0\nu\beta\beta$ claim, e.g., in terms of coexisting standard and nonstandard mechanisms with $m_{\beta\beta} \lesssim 0.2$ eV and $\Delta m_{\beta\beta} \gtrsim 0.1$ eV, respectively (but adding up to $m'_{\beta\beta} \sim 0.3$ eV); the same adjustment should then apply, within QRPA uncertainties, to the associated $0\nu\beta\beta$ signals in ^{82}Se , ^{100}Mo , and ^{130}Te .

We emphasize that our results refer to a specific set of four nuclei and four mechanisms, described within state-of-the-art QRPA nuclear structure calculations. Nondegenerate scenarios may well emerge for other $0\nu\beta\beta$ nuclei, mechanisms and observables, or if prospective NME estimates in QRPA (or in alternative nuclear models) can reach significantly higher accuracies. We plan to explore some of these possibilities in future works.

ACKNOWLEDGMENTS

The work of G. L. F., E. L., and A. M. R. is supported by the Italian Istituto Nazionale di Fisica Nucleare (INFN) and Ministero dell'Istruzione, dell'Università e della Ricerca (MIUR) through the ‘‘Astroparticle Physics’’ research project. A. F. and F.Š. acknowledge support of the Deutsche Forschungsgemeinschaft within the project 436 SLK 17/298. The work of F.Š. was also partially supported by the VEGA Grant agency of the Slovak Republic under Contract No. 1/0639/09.

Note Added.— The NME estimates used in this work for various mechanisms and QRPA variants (see Table I) are also being reported in another recent preprint [49], where they are analyzed within different scenarios for coexisting mechanisms (with detailed discussions of non-interfering cases [50] and/or of complex η 's), as well as with different aims and perspectives. The approaches used in our paper and in [49] are largely nonoverlapping, apart from the description of common NME inputs. The paper [49] analyzes what one can learn about the importance of the different mechanisms for the neutrinoless double beta decay, in particular, if accurate enough data and matrix elements will be available. The present paper shows that the current accuracy of the matrix elements does not prevent degeneracies and needs to be improved. One

will also need future data with smaller errors for $2\nu\beta\beta$ (to better constrain g_{pp}) and precise enough half-lives for $0\nu\beta\beta$ decays to discriminate between different mechanisms for the neutrinoless decay. Finally, concerning non-interfering cases [50], it should be noted that the associated equations would be of the form $\sum_i (M_i^j)^2 \eta_j^2 = \mu_i^2$ in the unknown η_j^2 [49]. Numerically, we find that the $(M_i^j)^2$ matrices and submatrices have reciprocal condition numbers about twice as large as the M_i^j (sub)matrices. However, since fractional differences due to different QRPA variants also double when $M_i^j \rightarrow (M_i^j)^2$, there is no net gain, and the η_j solutions remain unstable within current uncertainties.

-
- [1] K. Nakamura, S. T. Petcov, “Neutrino mass, mixing, and oscillations,” in K. Nakamura *et al.* (Particle Data Group), *J. Phys. G* **37**, 075021 (2010).
- [2] S. M. Bilenky, *Phys. Part. Nucl.* **41**, 690 (2010).
- [3] F. T. Avignone, III, S. R. Elliott, and J. Engel, *Rev. Mod. Phys.* **80**, 481 (2008).
- [4] W. Rodejohann, arXiv:1011.4942 [Nucl. Phys. B (Proc. Suppl.) (to be published)].
- [5] F. Šimkovic, J. Vergados, and A. Faessler, *Phys. Rev. D* **82**, 113015 (2010).
- [6] S. M. Bilenky and J. A. Grifols, *Phys. Lett. B* **550**, 154 (2002).
- [7] S. M. Bilenky and S. T. Petcov, arXiv:hep-ph/0405237.
- [8] F. Deppisch and H. Päs, *Phys. Rev. Lett.* **98**, 232501 (2007).
- [9] V. M. Gehman and S. R. Elliott, *J. Phys. G* **34**, 667 (2007); **35**, 029701(E) (2008).
- [10] G. L. Fogli, E. Lisi, and A. M. Rotunno, *Phys. Rev. D* **80**, 015024 (2009).
- [11] A. Faessler, G. L. Fogli, E. Lisi, V. Rodin, A. M. Rotunno, and F. Šimkovic, *Phys. Rev. D* **79**, 053001 (2009).
- [12] A. Faessler and F. Šimkovic, *J. Phys. G* **24**, 2139 (1998).
- [13] M. Doi, T. Kotani, and E. Takasugi, *Prog. Theor. Phys. Suppl.* **83**, 1 (1985).
- [14] R. N. Mohapatra and G. Senjanovic, *Phys. Rev. D* **23**, 165 (1981).
- [15] V. Tello, M. Nemevsek, F. Nesti, G. Senjanovic, and F. Vissani, *Phys. Rev. Lett.* **106**, 151801 (2011).
- [16] F. Šimkovic, G. Pantis, J. D. Vergados, and A. Faessler, *Phys. Rev. C* **60**, 055502 (1999).
- [17] R. N. Mohapatra, *Phys. Rev. D* **34**, 3457 (1986).
- [18] J. D. Vergados, *Phys. Lett. B* **184**, 55 (1987).
- [19] M. Hirsch, H. V. Klapdor-Kleingrothaus, and S. G. Kovalenko, *Phys. Rev. Lett.* **75**, 17 (1995).
- [20] A. Faessler, S. Kovalenko, F. Šimkovic, and J. Schwieger, *Phys. Rev. Lett.* **78**, 183 (1997).
- [21] A. Faessler, S. Kovalenko, and F. Šimkovic, *Phys. Rev. D* **58**, 115004 (1998).
- [22] M. Hirsch and J. W. F. Valle, *Nucl. Phys.* **B557**, 60 (1999).
- [23] H. Päs, M. Hirsch, H. V. Klapdor-Kleingrothaus, *Phys. Lett. B* **459**, 450 (1999).
- [24] V. A. Rodin, A. Faessler, F. Šimkovic, and P. Vogel, *Phys. Rev. C* **68**, 044302 (2003); *Nucl. Phys.* **A766**, 107 (2006) **A793**, 213(E) (2007).
- [25] F. Šimkovic, A. Faessler, V. Rodin, P. Vogel, and J. Engel, *Phys. Rev. C* **77**, 045503 (2008).
- [26] A. Wodecki, W. A. Kaminski, and F. Šimkovic, *Phys. Rev. D* **60**, 115007 (1999).
- [27] A. Faessler, T. Gutsche, S. Kovalenko, and F. Šimkovic, *Phys. Rev. D* **77**, 113012 (2008).
- [28] J. Menendez, A. Poves, E. Caurier, and F. Nowacki, *Nucl. Phys.* **A818**, 139 (2009).
- [29] P. K. Rath, R. Chandra, K. Chaturvedi, P. K. Raina, and J. G. Hirsch, *Phys. Rev. C* **80**, 044303 (2009).
- [30] D. S. Delion, J. Dukelsky, and P. Schuck, *Phys. Rev. C* **55**, 2340 (1997).
- [31] F. Krmpotic, E. J. V. de Passos, D. S. Delion, J. Dukelsky, and P. Schuck, *Nucl. Phys.* **A637**, 295 (1998).
- [32] F. Šimkovic, A. Faessler, and P. Vogel, *Phys. Rev. C* **79**, 015502 (2009).
- [33] M. K. Cheoun, A. Bobyk, A. Faessler, F. Šimkovic, and G. Teneva, *Nucl. Phys.* **A561**, 74 (1993).
- [34] F. Šimkovic, A. Faessler, H. Muther, V. Rodin, and M. Stauf, *Phys. Rev. C* **79**, 055501 (2009).
- [35] A. S. Barabash, *Proceedings of MEDEX'09, Workshop on Matrix Elements for the Double-beta-decay EXperiments (Prague, Czech Republic, 2009)*, edited by O. Civitarese, I. Stekl, and J. Suhonen, AIP Conf. Proc. Vol. 1180, 6 (2009).
- [36] A. Faessler, G. L. Fogli, E. Lisi, V. Rodin, A. M. Rotunno, and F. Šimkovic, *J. Phys. G* **35**, 075104 (2008).
- [37] J. W. Demmel, *Applied Numerical Linear Algebra* (SIAM, Philadelphia, PA, 1997), p. 419.
- [38] G. H. Golub and C. F. Van Loan, *Matrix computation* (Johns Hopkins Univ. Press, Baltimore, MD, 1996), p. 728.

- [39] E. Anderson *et al.*, *LAPACK User's Guide* (SIAM, Philadelphia, PA, 1994), p. 407, [website: www.netlib.org/lapack](http://www.netlib.org/lapack).
- [40] H. V. Klapdor-Kleingrothaus, I. V. Krivosheina, A. Dietz, and O. Chkvorets, *Phys. Lett. B* **586**, 198 (2004).
- [41] H. V. Klapdor-Kleingrothaus and I. V. Krivosheina, *Mod. Phys. Lett. A* **21**, 1547 (2006).
- [42] A. Ali, A. V. Borisov, and D. V. Zhuridov, *Yad. Fiz.* **73**, 2139 (2010) [*Phys. At. Nucl.* **73**, 2083 (2010)].
- [43] J. Menendez, A. Poves, E. Caurier, and F. Nowacki, *Nucl. Phys.* **A818**, 139 (2009).
- [44] J. Barea and F. Iachello, *Phys. Rev. C* **79**, 044301 (2009).
- [45] P. K. Rath, R. Chandra, K. Chaturvedi, P. K. Raina, and J. G. Hirsch, *Phys. Rev. C* **82**, 064310 (2010).
- [46] T. R. Rodriguez and G. Martinez-Pinedo, *Phys. Rev. Lett.* **105**, 252503 (2010).
- [47] Amand Faessler, [arXiv:1104.3700](https://arxiv.org/abs/1104.3700).
- [48] G. L. Fogli, E. Lisi, A. Marrone, A. Melchiorri, A. Palazzo, A. M. Rotunno, P. Serra, J. Silk, and A. Slosar, *Phys. Rev. D* **78**, 033010 (2008).
- [49] A. Faessler, A. Meroni, S. T. Petcov, F. Šimkovic, and J. Vergados, *Phys. Rev. D* **83**, 113003 (2011).
- [50] A. Halprin, S. T. Petcov, and S. P. Rosen, *Phys. Lett. B* **125**, 335 (1983).